THE ROOF STRUCTURES OF THE NEW SPORT HALL IN ATHENS: DESIGN, CONSTRUCTION AND PERFORMANCE

M MAJOWIECKI and F ZOULAS***

*Istituto di Tecnica delle costruzioni, Facoltà di Ingegneria
Università di Bologna, Italy

**Computer Aided Design Laboratory
Bologna, Italy

This work illustrates the general data of the structural design, the elaborations concerning the executive design, the construction details, the assembly technique and times and the cable structure pre-stressing operations used for the roof structures of the new sport hall in Athens.

1. GEOMETRICAL AND MECHANICAL CHARACTERISTICS OF THE ROOF STRUCTURE

After drawing up the executive architectural design (Fig 1, see Appendix 1), the geometrical and mechanical data necessary for the structural analysis were defined.

1.1. The suspended roof

The roof structure consists of an orthogonal rope net, whose average surface can be defined geometrically as a saddle surface with total negative curvature, very similar to that of a hyperbolic paraboloid. The main data of the cable structure are:

1.1.1. Diameter: 113.96 m (R = 56.98 m).

1.1.2. Upper rope diameter: Ø 60 mm (Fe = 21.106 cm^2); construction 127 x 4.6; σ_{ult} = 1600 N/mm^2.
Lower rope diameter: Ø 46 mm (Fe = 12.784 cm^2); construction 127 x 3.6; σ_{ult} = 1600 N/mm^2.
Elasticity modulus of the ropes: E = 165 KN/mm^2.

1.1.3. Mesh dimensions: 4.00 x 4.00 m

1.1.4. Equation of the cable net boundary (anchorage line)

The anchorage ring line is defined geometrically by the intersection between a circular vertical cylinder of diameter 113.96 m, which is the maximum free span of the cable net structure, and a hyperbolic paraboloid co-axial to it.

The position of the theoretical anchorage points of the cable structure is expressed analytically by:

$$\begin{cases} \dfrac{6.15}{56.98^2}(x^2 - y^2) + 28.74 = Z \\ x^2 + y^2 = 56.98^2 \end{cases} \qquad \ldots\ldots 1.$$

The geometrical co-ordinates of the discrete anchorage points of the ropes are so determined on the ring, according to a Cartesian axes system, considering

x axis directed to the upper point (H = +34.89);
y axis directed to the lower point (H = +22.59);
z axis directed upwards.

1.2. Cable net mesh-comparative cost analysis

The cable structural distribution in plan has been definitely decided according to a net mesh of 4x4 m after a careful analysis of both the cost of supply of the roof materials, and the cost of the erection and pre-stressing of the cable structure.

The results of the comparative economic analysis between the two net mesh solutions 4x4 m a,d 2x2 m are submitted up in Table 1. Considering the solution with net 4x4 m as the comparative unit price cost, it is possible to deduce from Table 1 that the two solutions are equivalent as far as the total cost of supply of the roof materials is concerned. On the contrary, the costs of erection and pre-stressing of the rope net structure are considerably different.

In fact, with a net mesh of 4x4 m, although the steel consumption for the ropes and the cost of the covering remain about the same, the cost of erection of the structure joint-locks is four times less; while the erection of the ropes and the stretching operation are halved.

TABLE 1

Solution	Rope supply	Roof covering (supply, erection)	Erection and prestressing of the net
2 x 2	1.05	0.923	2 ÷ 2.5
4 x 4	1	1	1

1.3. The peripheral ring

The border structure, to which the rope net is anchored, consists of a perimetrical box-section ring in pre-stressed rein-

forced concrete which follows the movement of the border curve, Eqn 1.

1.3.1. Geometry of the beam axis

The downview of the beam axis is a circle with a radius R = 61.66 m. The supports are located in downview on a circle with a radius R_1 = 61.50 m in angular distance α_o = 11.25°. The support heights are defined on the basis of the heights of the corresponding peripheral points of the suspended roof, located on the same radial direction, with a -5.45 m difference in height.

The structure of the anchorage ring is defined in space by moving the plane frame defining the external contourn of the section, resting on the generatrix determined by Eqn 1 keeping the plan, containing this section, vertical.

The maximum gradient between the points of the border line, defining the anchorage structure, is 12.3 m equal to about 11% of the free span.

1.3.2. Cross-sections (on vertical plane)

The moments of inertia and section area are variable due to the modification of the thickness of the walls of which the structure consists. The standard sections, which form the various elements between two consecutive supports of the ring, are shown in Fig 2.

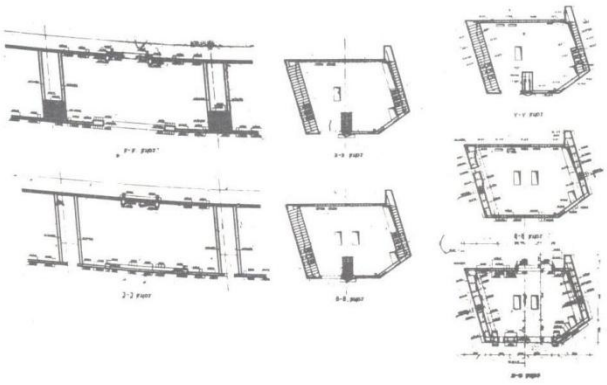

Fig 2

The area and inertia properties of the ring sections are:

- Cross-section A (without openings):

$F = 9.0705\ m^2$

$J_r = 34.427\ m^4$

$J_z = 103.6281\ m^4$

$J_D = 63.0817\ m^4$

- Cross-section B (with openings):

$F = 8.9219\ m^2$

$J_r = 32.59444\ m^4$

$J_z = 104.08146\ m^4$

$J_D = 63.0817\ m^4$

- Cross-section A (segments between supports 7-8-8-7)

$F = 10.5913\ m^2$

$J_r = 39.7864\ m^4$

$J_z = 121.7072\ m^4$

$J_D = 63.0817\ m^4$

1.3.3. Materials

Concrete B 450
Elasticity modulus: E_i = 35 KN/mm²;
E(t) according to time schedule
Shear modulus: G = 15 KN/mm².
Poisson ratio: ν = 0.167.

1.4. The ring supporting system

The supports are placed in relation to the frames supporting the stands. These frames, which are radial and concentric as regards the centre of the construction, are also made of pre-stressed reinforced concrete and are of variable height in order to altimetrically follow the movement of the border ring.

The supporting system is also equipped with hydraulic jacks, which allow the horizontal displacements due to elastic deformations and hinder the eventual movements of the rigid body of the ring, due to seismic action.

1.4.1. Factors of elastic settlements of the supports

Support 1: $W_1 = 6.6757 \times 10^{-3}$ m/1000 KN
" 2: $W_2 = 9.0127 \times 10^{-3}$ "
" 3: $W_3 = 7.2191 \times 10^{-3}$
" 4: $W_4 = 5.2207 \times 10^{-3}$ "
" 5: $W_5 = 3.7959 \times 10^{-3}$ "
" 6: $W_6 = 2.7205 \times 10^{-3}$ "
" 7: $W_7 = 1.7006 \times 10^{-3}$ "
" 8: $W_8 = 0.6432 \times 10^{-3}$ "

1.4.2. Absolute support settlements

	max W	min W
Support 1:	-1.095×10^{-3} m	$+0.2944 \times 10^{-3}$ m
" 2:	-2.359×10^{-3} m	$+0.1366 \times 10^{-3}$ m
" 3:	-1.9517×10^{-3} m	$+0.0787 \times 10^{-3}$ m
" 4:	-1.3280×10^{-3} m	-
" 5:	-0.8161×10^{-3} m	-
" 6:	-0.5202×10^{-3} m	-
" 7:	-0.2534×10^{-3} m	-
" 8:	-	-

2. LOADING ANALYSIS

2.1. Cable structure

		Load-Code
Dead load of the ropes	90 N/m²	[a]

Dead load of the covering and additional permanent loadings	360 N/m^2	[b]
Snow loading	650 N/m^2	[c]
Wind loading (c = -0.8)	1100 N/m^2	[d]

2.2. Border ring

Dead weight of the ring	216 KN/m	[e]
Pre-stressing variable between two consecutive elements of the ring	(see Table 2)	[f]
Additional permanent loadings	14 KN/m	[g]
Accidental loadings	458 KN/m	[h]

TABLE 2

Element number	Prestressing axial force (MN)	Horizontal eccentricity (m)	Vertical eccentricity (m)
1	33.50	0.93	1.08
2	33.50	0.93	1.08
3	30.00	0.775	0.90
4	23.00	0.465	0.54
5	12.50	0	0
6	26.00	-0.2	0.50
7	35.00	-0.3	0.84
8	39.50	-0.4	1.04
9	39.50	-0.4	1.01

2.3. Loading combinations

The loading combinations, leading to the definite statical verifications of the covering structures, have been determined according to the maximum stresses and deformations, and to the various constructive phases, in accordance with a pre-set time schedule.

In accordance with the time-schedule illustrated in Table 3, the influence of the reologic deformations E(t) of the perimetrical ring has been duly considered for the various possible loading combinations.

TABLE 3

Month	1st	2nd	3rd	4th	5th	6th	7th	8th	9th
Ring Performance									
Ring prestressing									
Cable-structure Erection									
Cable-structure pre-tension									
Covering performance									

The static loading combinations considered are:

1) [e]
2) [e] + [f]
3) [e] + [f] + [a]
4) [e] + [f] + [g] + [a] + [b]
5) [e] + [f] + [g] + [h] + [a] + [b] + [c]
6) [e] [f] + [g] + [a] + [b] + [c]

The thermal variations have been considered associated to the conditions of maximum loading 5) and 6), in accordance with the following groups:

GROUP I

- Temperature difference between the lower and upper faces of the ring:

$$t_i - t_s = -15\ ^\circ C$$

- Temperature difference between the internal and external faces of the ring:

$$t_i - t_e = -15\ ^\circ C$$

- Temperature difference acting on the cable-structure:

$$\Delta T = -10\ ^\circ C$$

GROUP II

$$t_i - t_s = 15\ ^\circ C$$
$$t_i - t_e = 15\ ^\circ C$$
$$\Delta T = +10\ ^\circ C$$

GROUP III

Concrete shrinkage: equivalent to $t_s = -15\ ^\circ C$.

3. THE STRUCTURAL SCHEME AND THE MATHEMATICAL MODEL

Taking advantage of the two symmetry axes, only a quarter of the ring has been considered and schematized as a space frame. The joints of this space frame have been defined principally, in correspondence to the rope anchorages, at the beginning and end of the ring section variation and in correspondence to its supports. These supports elasticity and non-elastically yielding are eccentric with regard to the ring barycentric axis.

The rope anchorages are located at the ring upper plate. The cable structure is outlined as a system of bar-joints with the possibility of transmitting only tensile forces ($S > 0$) and consists of 167 internal joints having 3 degrees of freedom, 130 border joints and 385 bar elements, Fig 3.

According to the structural arrangement, the cable structure interacts elastically with the border ring for all loading combinations.

In order to obtain more detailed information for the actual stress distribution the ring has been verified by means of a finite element analysis. Figures 4 and 5 show the plane and axonometric view of the finite element mesh schematization for the ring actual structure.

The organisation of the global calculation programme implies therefore three principal groups (routines) of resolution:

- Programme rete, for the research of state "0";

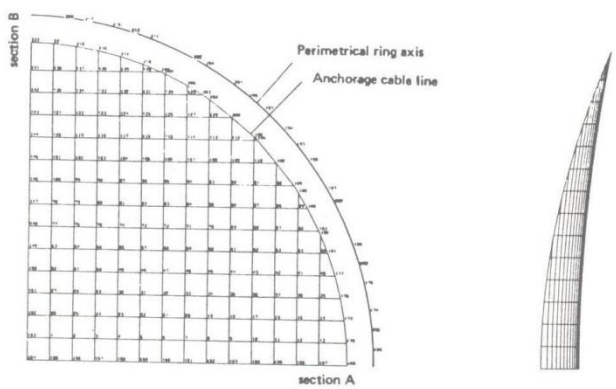

Fig 3 Automatic output plotter of the rope net mesh and border ring.

- Programme tenso/tensodin, for the statical and dynamical analysis of the cable structure;
- Programme of space frame analysis (S.F.A.) or finite element analysis (F.E.A.) for the static analysis of the border ring.

The state "0" is obtained with the method outlined in Ref 2; the statical and dynamical analysis are computed with the mixed substructuring method of Ref 3, taken into account the interaction between ring and cable structures.

In the flow-chart illustrated in Fig 6 the global organization of the computer programme utilized for the structural analysis is synthetically shown.

4. THE RESULTS

4.1. State "0"

The loadings combination no. 3 has been chosen for the definition of the state "0" of the structural system-border ring and cable structure.

The horizontal components of the stresses in the primary and secondary ropes have been fixed in the pre-stressing state to:

$H_p = 582$ KN

$H_s = 615$ KN

4.2. States of maximum stress and deformation (verification)

The loading combinations no. 5 and no. 6 correspond to the snow loading and wind loading on the covering respectively. The ring has been designed in order to fit the best flexural distribution permitted by the bond represented by the displacement limitation of $\Delta f \leq 0.005\ L$ (L = maximum free span).

The maximum tensile strength in the primary ropes for the snow loading combination is equal to 1210 KN, while in the secondary ropes for the wind loading combination is equal to

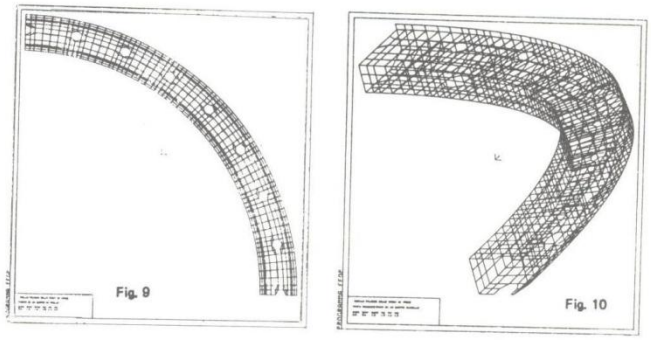

Finite element mesh schematization for the ring structure. Input geometrical data for computer programme.

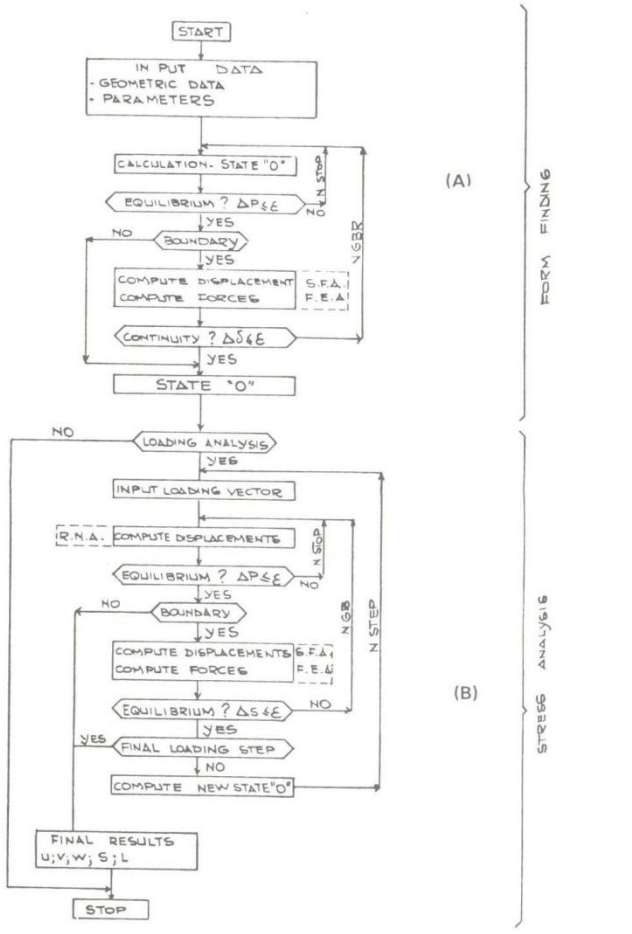

Fig 6 FLOW CHART - form finding and stress analysis.

810 KN.

According to what mentioned above, Fig 7 shows the final plotted diagram of axial forces, shear and moments for the snow condition (with the correspondin associated group of thermal variations in a quarter ring), obtained as output of the space frame analysis program.

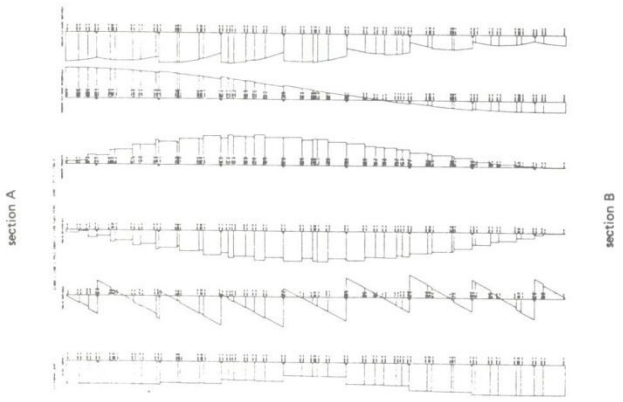

Fig 7 SNOW LOAD - automatic plotter of stresses in quarter ring.

On the basis of the stresses obtained for the different loading combinations, the stresses on the prestressed reinforced concrete ring section have been verified. Figure 8 shows the variation of the pression center and the neutral axis for single and combined loadings in the most stressed section of the ring. The verifications have been computed interactively with a stress analysis program on flexural and normally loaded sections.

The maximum stresses computed have been compared by means of a more precise analysis via finite elements, thus obtaining an excellent result check and detailed information on the stress state around the numerous holes and concentrated load in the ring. The following peaks were found in the second loading combination:

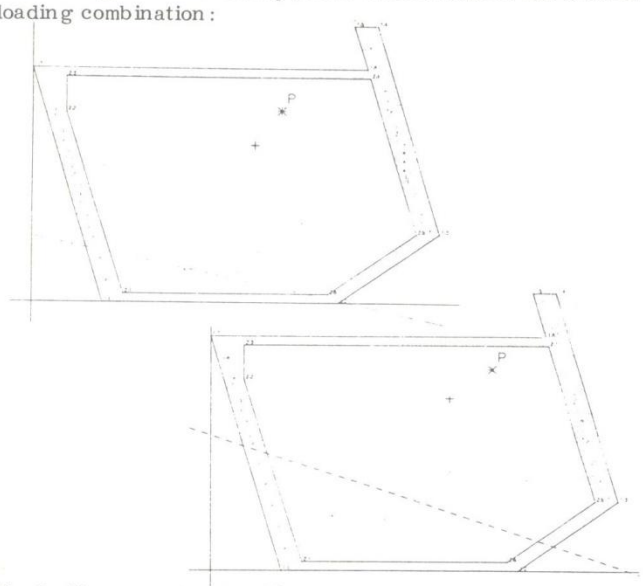

Fig 8 Stress control modification in the ring section.

SIGMA C = -13.5 MPa
SIGMA F = 14.2 MPa

5. CONSTRUCTION DETAILS

5.1. Rope anchorages

The rope transmit the anchorage forces to the border ring via four Dywidag bars Ø 32 ST 80/105, anchored in turn on the upper plate of the ring. The detail connecting the rope to the Dywidag bars should allow:

a) an easy adjustment so as to avoid geometric execution errors;
b) the possibility of connecting hydraulic jacks for the introduction of the state "0" forces;
c) the spheric rotation of the anchorage cable heads to adapt to the angular variations due to the different loading combinations.

In order to attain these aims, the detail illustrated in Fig 9 (see Appendix) has been designed.

The parts composing the rope anchorage detail have been tested experimentally by means of fracture tests. The safety factors obtained are very high if a considerable rigidity of the detail is also to be obtained so as to minimize the elastic deformation. Some results are illustrated in Fig 10, see Appendix.

5.2. Rope-rope connection

The purpose of the rope-rope connection is to absorb the friction tangential stresses,which are very limited and allow us to obtain a very simple detail realized in aluminium, Fig 11 (see Appendix).

5.3. Covering

In the executive design special attention has been paid to the covering which is composed of:

- corrugated sheat (HACIERCO), 106 mm high and 10/10 mm thick, painted on the lower side and galvanized on the upper side, with 750 mm pitch and resting on the secondary ropes every 4 m. The sheet is connected to the ropes by means of cadmium plated U bolts;
- vapor barrier SARNAVAP 1000;
- rigid heat insulator, 6 cm thick, having a coefficient of heat conductivity K = 0.6 kcal/h m^2;
- polyester and PEC waterproofing membrane;
- screw connecting the insulating and waterproofing layers to the corrugated sheet.

The executive designs of the detail are illustrated in Fig 12 (see Appendix).

6. ERECTION AND POSITIONING OF THE CABLE STRUCTURES

The primary ropes have been positioned according to the scheme of Fig 13 (see Appendix) by means of cranes in order to decrease the horizontal forces next to the winches.

The secondary ropes have been positioned by sliding them on the primary ropes according to the method illustrated in Fig 14 (see Appendix).

6.1. Description of the pre-stressing operations

The purpose of the pre-stressing operations on the rope net is to attain the tensile and geometric state referred to in theory as "STATE 0".

During the erection of the rope net the following operations have been considered:

- positioning of the anchorage cable heads of the secondary ropes according to the theoretical results;
- positioning of the anchorage cable heads of the primary ropes on the threaded bars in a known point.

The stress state predicted for the rope net in STATE "0" has been obtained by means of an iterative pre-stressing procedure according to conservative phases, as shown in the following:

PHASE 1 - Removal of the big kinematic displacements by acting on the adjustable anchorage points of the primary ropes.

PHASE 2 - Optical instrumental measurement and control of the positioning of the secondary rope anchorage points; control and quantification of the positioning errors of the anchorage boxes; modification of th position of the secondary rope anchorage points according to the above errors.
NOTE: The correction is possible only along the rope direction. No correction is possible transversally to the rope axis.

PHASE 3 - Introduction of a first stress level (first elastic phase) in accordance with the theoretical results.

PHASE 4 - Instrument measurement of the actual position of the primary rope anchorage points; control and quantification of the displacement of the primary rope anchorage cable heads to be carried out during the subsequent phases.

PHASE 5 - Introduction of a second stress level (second elastic phase) in accordance with the theoretical results.

PHASE 6 - Local action on some ropes in order to minimize the influence of the longitudinal and transversal border errors on the positioning of the anchorage points in the concrete ring structure.

The pre-stressing steps have been numerically simulated according to the same program illustrated in section 3, by "relaxing" the ropes in accordance with the pre-established sequence. In this way the enclosed pre-stressing tables have been obtained (Tables 4, 5 and Fig 15).

In the case of temperature differences recorded in the building site with respect to the rope cut mean temperature, the pre-stressing stresses have been duly modified according to a suitable Table 6.

The erection and pre-stressing of the rope net were concluded on August 1983, according to PERT time schedule (Appendix, Fig 16).

		PRIMARY CABLES													
STEP 1		P_{14}	P_{13}	P_{12}	P_{11}	P_{10}	P_9	P_8	P_7	P_6	P_5	P_4	P_3	P_2	P_1
P	From	14,5	20,5	23,4	26,2	27,5	28,8	29,7	30,5	31,0	31,4	31,5	31,5	29,6	21,6
	To	39,6	44,1	48,5	50,7	52,9	54,5	56,1	57,3	58,4	58,9	59,4	58,4	55,1	49,4
Δl	From	530	518	509	503	498	491	484	484	478	478	487	486	486	486
	To	547	541	537	534	533	528	524	525	522	522	531	531	531	531
	f	17	23	28	31	35	37	40	41	44	44	44	45	45	45

STEP 2		P_{14}	P_{13}	P_{12}	P_{11}	P_{10}	P_9	P_8	P_7	P_6	P_5	P_4	P_3	P_2	P_1
P	From	34,6	36,8	37,9	38,4	39,9	39,1	39,3	39,5	39,6	39,7	39,8	39,2	37,2	29,4
	To	60,9	62,7	63,6	64,3	65,2	66,2	67,1	67,6	68,5	68,5	68,2	67,0	63,7	58,0
Δl	From	547	541	537	534	533	528	524	525	522	522	531	531	531	531
	To	563	565	564	565	567	564	563	566	565	565	575	575	575	575
	f	16	24	27	31	34	36	39	41	43	43	44	44	44	44
SEQUENCE		1	2	3	4	5	6	7	8	9	10	11	12	13	14

P = pre-stressing force (ton.)
Δl = elastic deformation.

STEP 2	PRE - STRESSING FORCE MATRIX IN PRIMARY CABLES														
PRE STRESSING SEQUENCE	P_{14}	P_{13}	P_{12}	P_{11}	P_{10}	P_9	P_8	P_7	P_6	P_5	P_4	P_3	P_2	P_1	z
0	34,6	38,6	41,6	43,5	45,1	46,1	46,7	47,8	47,9	48,8	49,0	49,2	49,4	49,4	27,82
1	60,9	36,8	40,8	43,1	44,8	46,0	46,7	47,8	47,9	48,8	49,0	49,2	49,5	49,4	27,82
2	57,5	59,4	63,6	38,4	42,7	44,8	46,1	47,6	47,9	48,9	49,3	49,6	49,8	49,6	27,82
3	57,5	59,4	63,6	38,4	42,7	44,8	46,1	47,6	47,9	48,9	49,3	49,6	49,8	49,6	27,81
4	56,8	57,9	59,9	64,3	39,9	43,2	45,2	47,2	47,7	49,0	49,4	49,7	49,9	50,0	27,81
5	56,4	56,9	58,2	60,3	65,2	39,1	43,5	46,2	47,3	48,8	49,4	49,8	50,1	50,0	27,81
6	56,3	56,6	57,3	58,7	60,9	66,2	39,3	44,0	46,8	48,0	49,2	49,8	50,0	50,0	27,81
7	56,1	56,3	56,7	57,6	59,1	61,4	67,1	39,5	44,5	47,3	48,7	49,5	50,1	50,2	27,81
8	56,1	56,2	56,6	57,1	58,1	59,6	61,9	67,8	39,6	45,0	47,4	48,7	49,2	49,9	27,82
9	56,2	56,2	56,4	56,8	57,5	58,5	60,1	62,3	68,5	39,7	45,5	47,5	48,7	49,0	28,82
10	56,4	56,4	56,5	56,8	57,3	58,0	59,0	60,4	62,8	68,5	39,8	45,3	47,0	47,4	27,85
11	56,5	56,6	56,6	56,9	57,2	57,7	58,4	59,3	60,8	62,7	68,2	39,2	44,1	45,0	27,87
12	56,6	56,7	56,8	57,0	57,3	57,6	58,1	58,5	59,5	60,5	62,1	67,0	37,2	40,6	27,90
13	56,8	57,0	57,2	57,3	57,4	57,6	57,9	58,0	58,5	58,8	59,3	60,1	63,7	29,4	27,97
STATE'0' 14	56,8	57,0	57,2	57,3	57,5	57,6	57,8	57,8	58,0	58,0	58,0	58,0	58,0	58,0	28,00

" FORCE VARIATIONS IN STATE '0' DUE TO ΔT"

	PRIMARY CABLES														
T	P_1	P_2	P_3	P_4	P_5	P_6	P_7	P_8	P_9	P_{10}	P_{11}	P_{12}	P_{13}	P_{14}	f cm
± 5°	1,38	1,38	1,38	1,38	1,38	1,40	1,42	1,44	1,48	1,49	1,59	1,67	1,78	1,91	0,7
± 10°	2,76	2,78	2,77	2,80	2,82	2,85	2,88	2,93	3,00	3,09	3,19	3,43	3,55	3,84	1,5
± 15°	4,17	4,18	4,18	4,21	4,24	4,30	4,34	4,42	4,53	4,65	4,82	5,09	5,35	5,78	2,2
± 20°	5,58	5,58	5,59	5,62	5,67	5,67	5,76	5,81	5,91	6,06	6,21	6,75	7,14	7,71	2,9
± 30°	8,40	8,41	8,42	8,49	8,55	8,66	8,76	8,93	9,13	9,37	9,72	10,18	10,76	11,59	4,4

" FORCE VARIATION IN THE STATE '0' DUE TO ΔT"

	SECONDARY CABLES													
T	S_1	S_2	S_3	S_4	S_5	S_6	S_7	S_8	S_9	S_{10}	S_{11}	S_{12}	S_{13}	S_{14}
± 5°	1,70	1,73	1,72	1,71	1,70	1,68	1,65	1,63	1,60	1,55	1,51	1,47	1,42	1,35
± 10°	3,41	3,41	3,40	3,39	3,36	3,33	3,28	3,23	3,16	3,10	3,01	2,93	2,83	2,71
± 15°	5,09	5,1	5,08	5,06	5,02	4,98	4,91	4,84	4,74	4,65	4,52	4,39	4,25	4,07
± 20°	6,78	6,78	6,76	6,73	6,68	6,63	6,53	6,44	6,31	6,19	6,02	5,85	5,66	5,42
± 30°	10,16	10,15	10,12	10,07	10,00	9,92	9,76	9,63	9,45	9,25	9,02	8,77	8,48	8,13

ΔT = temperature changement from average temperature during rope cutting.

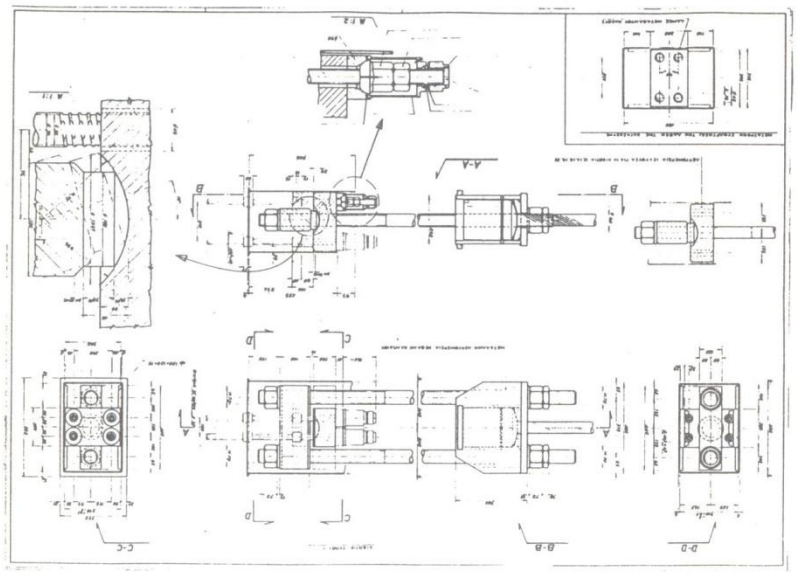

Fig. 9 Cable head detail

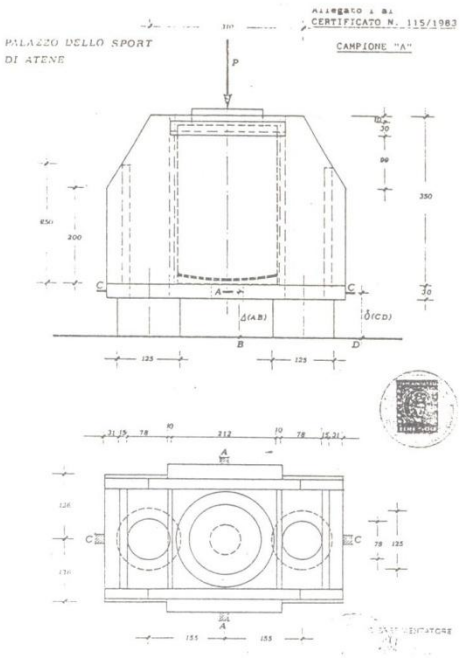

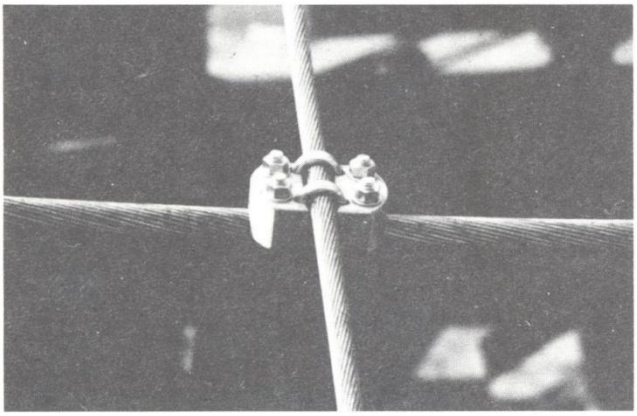

Fig. 11 Rope - rope friction detail

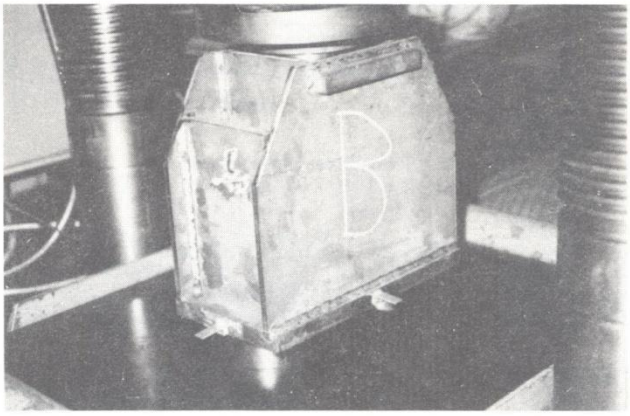

Fig. 10 Experimental analysis

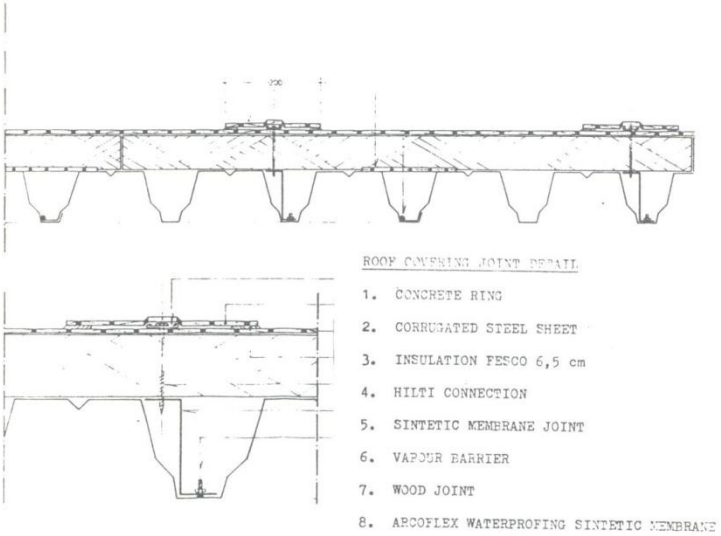

ROOF COVERING JOINT DETAIL

1. CONCRETE RING
2. CORRUGATED STEEL SHEET
3. INSULATION FESCO 6,5 cm
4. HILTI CONNECTION
5. SINTETIC MEMBRANE JOINT
6. VAPOUR BARRIER
7. WOOD JOINT
8. ARCOFLEX WATERPROFING SINTETIC MEMBRANE

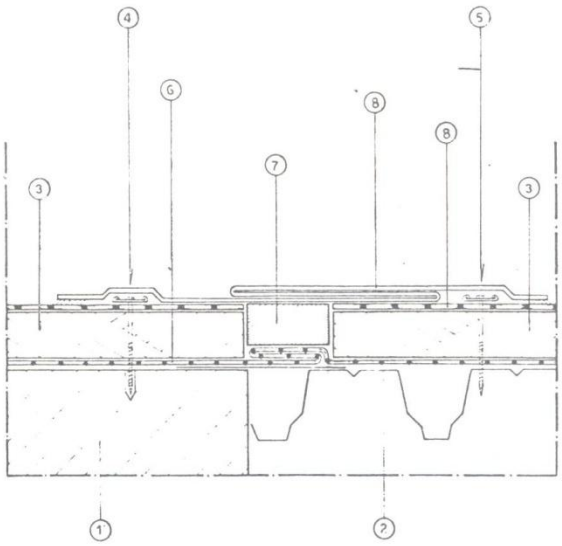

Fig. 12 Roof covering sandwich

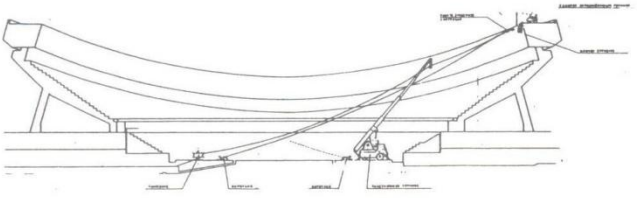

Fig. 13 Primary ropes erection

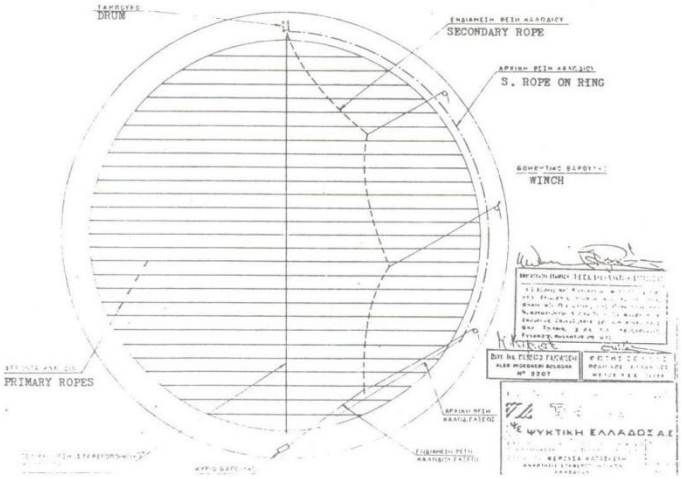

Fig. 14 Secondary ropes erection

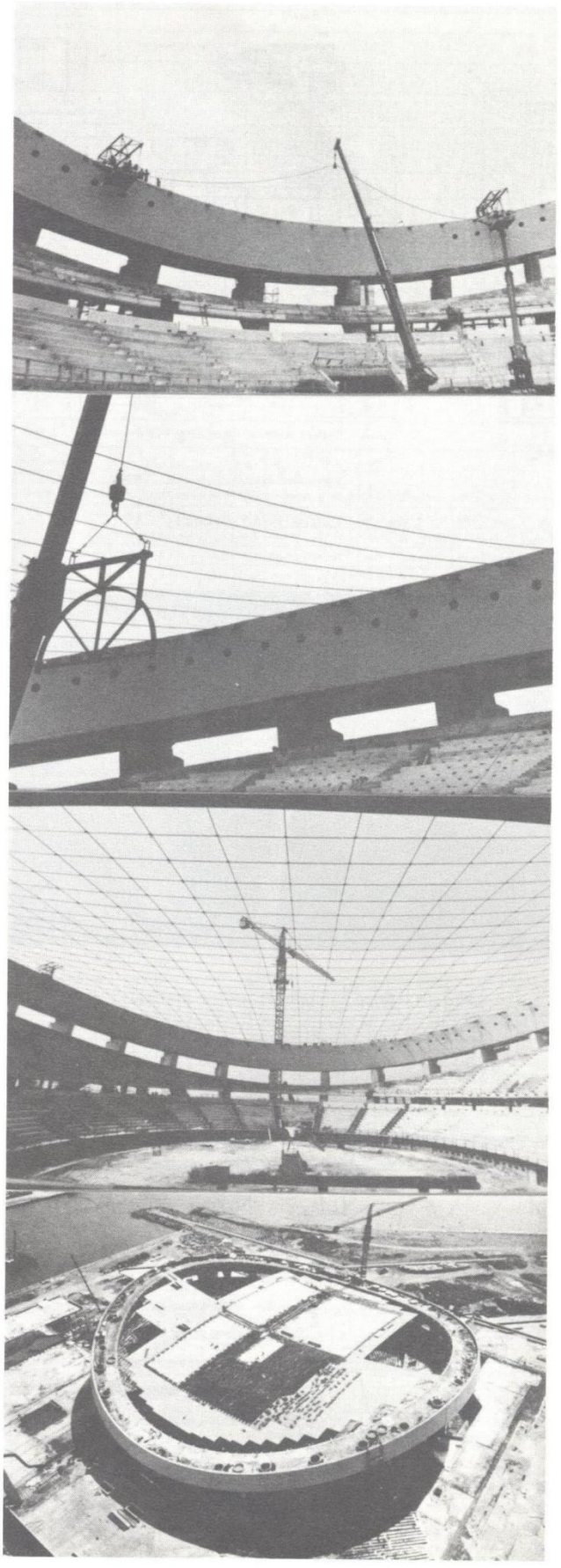

Fig. 16 PERT time

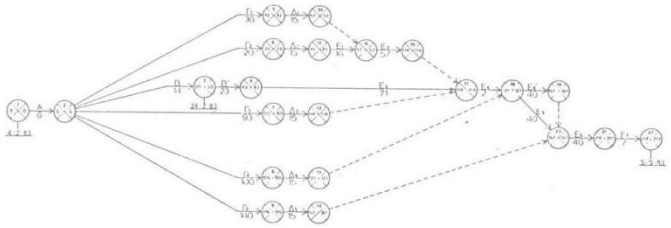

LIST OF ACTIVITIES
A. MEASUREMENTS OF ANCHORAGES COORDINATES
B. SHOP DRAWINGS
B'. APPROVAL OF SHOP DRAWINGS
C. PLACING OF ORDER WITH THE MATERIAL MANUFACTURERS
C1. CABLES
C2. ANCHORAGE SYSTEMS
C3. CORRUGATED STEEL SHEETS
C4. INSULATION MATERIAL
C5. WATERPROOFING MEMBRANE
D. ARRIVAL OF MATERIALS AT SITE
D1. CABLES
D2. ANCHORAGE SYSTEMS
D3. CORRUGATED STEEL SHEETS
D4. INSULATION MATERIAL
D5. WATERPROOFING MEMBRANE
EXXX E. ERECTION WORK
E1. ANCHORAGE SYSTEMS
E2. CABLES - PRESTRESSING OF THE NET
E3. END SUPPORTS OF STEEL SHEET
E4. - E'4. STEEL SHEETS
E5. VAPOR-BARRIER - INSULATION
E6. WATERPROOFING MEMBRANE
E7. MISCELLANEOUS

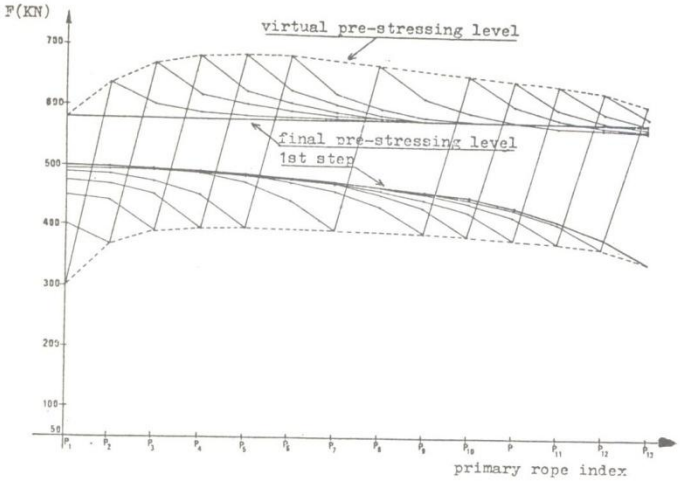

Fig. 15 Pre - stressing diagramm

ACKNOWLEDGEMENTS

Owner: General Secretariat of Athletics - Greece.
Architectural design: Archs T Papayiannis, J Baibas, A Gamini, M Koutsouna.
Structural design: Engrs D Bairaktaris, F Caridakis.
Roof structure calculations: Engrs R Alessi, M Majowiecki, F Zoulas.
Main contractors for the complete roof structure: Joint-Venture TECI SpA - Psyktiki Hellados S A.
Contractor's consultants on the roof structure: Engrs M Majowiecki, F Zoulas.
Main contractor for the civil, architectural and electromechanical works of sports hall: Archirodon Hellas S A.

REFERENCES

1. R ALESSI, D BAIRAKTARIS, F CARIDAXIS, M MAJOWIECKI, F ZOULAS, The roof structures of the new sports arena in Athens. World Congress on shell and spatial structures, September 1979, Madrid, Spain.
2. M MAJOWIECKI, G TIRONI, Geometrical configuration of tent and pneumatic structures obtained by interactive computer aided design, IASS World Congress, Montreal, 1976.
3. M MAJOWIECKI, Analisi interattiva di tensostrutture a rete, acciaio, no 9, 1982.

APPENDIX